Short Communication

Electroporation of outer membrane vesicles derived from *Pseudomonas aeruginosa* with gold nanoparticles

Zeineb Ayed[1,2] · Luana Cuvillier[3] · Garima Dobhal[4] · Renee V. Goreham[4]

Received: 21 August 2019 / Accepted: 7 November 2019 / Published online: 12 November 2019

Abstract
Since their discovery, extracellular vesicles have gained considerable scientific interest as a novel drug delivery system. In particular, outer membrane vesicles (OMVs) play a critical role in bacteria–bacteria communication and bacteria–host interactions by trafficking cell signalling biochemicals (i.e. DNA, RNA, proteins). Although previous studies have focused on the use of OMVs as vaccines, little work has been done on loading them with functional nanomaterials for drug delivery. We have developed a novel drug delivery system by loading OMVs with gold nanoparticles (AuNPs). AuNPs are versatile nanoparticles that have been extensively used in disease therapeutics. The particles were loaded into the vesicles via electroporation, which uses an electric pulse to create a short-lived electric field. The resulting capacitance on the membrane generates pores in the lipid bilayer of the OMVs allowing AuNPs (or any nanoparticle under 10 nm) inside the vesicles. Closure of the pores of the lipid membrane of the OMVs entraps the nanoparticles as cargo. Transmission electron microscopy was used to confirm the loading of AuNPs inside the OMVs and dynamic light scattering (DLS) and cryogenic scanning electron microscopy (cryo-SEM) verified the size and integrity of the OMVs. This is the first report to load nanoparticles into OMVs, demonstrating a potential method for drug delivery.

Electronic supplementary material The online version of this article (https://doi.org/10.1007/s42452-019-1646-2) contains supplementary material, which is available to authorized users.

✉ Renee V. Goreham, renee.goreham@newcastle.edu.au; Zeineb Ayed, zeineb.ayed@vuw.ac.nz | [1]The MacDiarmid Institute, Wellington 6012, New Zealand. [2]School of Chemical Physical Sciences, Victoria University of Wellington, Kelburn, Wellington 6012, New Zealand. [3]Graduate School of Chemistry, Physics and Biology of Bordeaux, 33000 Bordeaux, France. [4]School of Mathematical and Physical Sciences, University of Newcastle, Callaghan, NSW 2308, Australia.

Graphic abstract

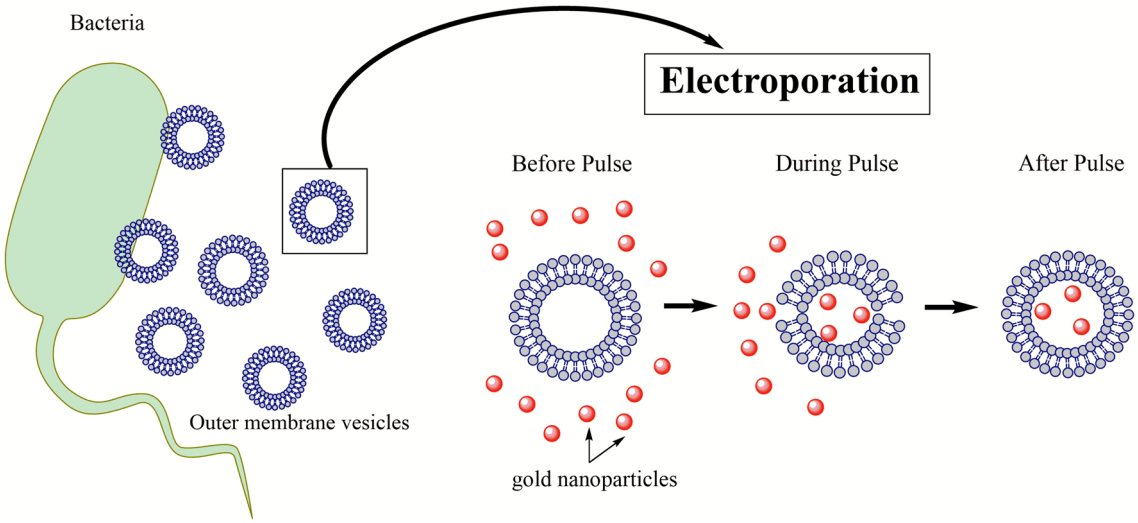

Keywords Extracellular vesicle · Drug delivery · Nanoparticle · Electron microscopy · Exosomes

1 Introduction

Living cells, such as bacteria, may hold the answer to superior transport of drug delivery with higher efficiencies and biocompatibility. Efficient-targeted drug delivery methods that have minimal immunogenic and toxic effects remain a primary challenge [1]. Among nanosized carriers that are applicable as drug delivery systems for cancer therapy are custom synthesised nanoparticles and cell-derived extracellular vesicles. Advances in nanotechnology have contributed to improved drug delivery strategies using materials such as quantum dots, AuNPs and carbon nanotubes [2–4]. Their small size provides advantages with cell penetration, and their ability to be functionalised makes further conjugation to drugs or targeting moieties easier [5]. However, some barriers such as biocompatibility, toxicity, and cost-effectiveness have hindered the clinical use of nanoparticles.

Cell-derived extracellular vesicles, such as exosomes derived from mammalian cells and OMVs derived from gram-negative bacteria, have shown promise in the area of drug delivery. Extracellular vesicles are non-toxic, biodegradable and can be programmed to target cells of interest [6]. Similar to the cell of origin, extracellular vesicles have a phospholipid bilayer membrane and are able to transmit information in the form of DNA, RNA and proteins and hence deliver cargo across long distances [7]. Exosomes have been investigated as biocompatible and targeted drug delivery vehicles but are expensive to cultivate and are usually isolated in lower concentrations compared to bacteria-derived extracellular vesicles [8]. In contrast, bacteria-derived extracellular vesicles including OMVs are cheaper to culture and can be isolated with higher yields. OMVs are vesicles that are spontaneously released from gram-negative bacteria, such as *Pseudomonas aeruginosa* and *Acinetobacter baumannii*. Increasing research on OMVs has focused on their applicability in vaccine development or as nature's own drug delivery vehicle [9].

Two main methods have been used for loading drugs into the mammalian extracellular vesicles, incubation and electroporation. Incubation of exosomes with curcumin showed that after 5 min, drug loading was successful and mediated significant anti-inflammatory effects in several disease models [10, 11]. Curcumin is known to cause lipid rearrangement and fluidity of the cell membrane, which may increase drug loading. A similar strategy using nanoparticles would not be possible due to their size and composition. However, electroporation has been shown to be an effective method to temporarily permeabilise the bilayer membrane of cells or extracellular vesicles and load drugs or other small molecules. Alvarez-Erviti et al. [12] first demonstrated the ability to load exosomes with siRNA to cross the blood–brain barrier. Since then, many researchers have demonstrated similar drug or nanoparticle loading, using electroporation to create pores within the exosome membrane [13, 14]. Doxorubicin (a chemotherapy drug) has also been loaded into exosomes via electroporation and delivered to target cells [10, 11, 15]. More recently, electroporation has been used to load nanoparticles into exosomes as a potential method for drug

delivery [16, 17]. With that said, there has been only two reports of electroporation of nanoparticles into mammalian-derived extracellular vesicles using Ag_2Se quantum dots or superparamagnetic iron oxide nanoparticles. There have been no previous reports on electroporation of bacteria-derived OMVs to load nanoparticles.

Herein, small AuNPs (~ 5 nm) were loaded into OMVs derived from *Pseudomonas aeruginosa* (PA01) via electroporation, as a potential mode of drug delivery. The stability of the OMVs before and after electroporation was investigated and compared using various methods such as DLS and electron microscopy. The stability of the AuNPs was further verified using UV–Vis absorption. Bacteria-derived OMVs were loaded with nanoparticles for the first-time using electroporation that could offer a versatile and novel method for customised drug delivery.

2 Experimental section

2.1 Materials

Tetrachloroauric(III) acid ($HAuCL_4{\cdot}3H_2O$, > 99.99% metals basis, Sigma-Aldrich, US), milli-Q water (resistivity of 18.2 MΩ cm), tannic Acid (Pure Science Ltd., New Zealand), sodium citrate (≥ 99%, Sigma-Aldrich, US), potassium carbonate (> 99.99% ACS grade, BDH chemicals), uranyl acetate (TAAB Labs), glycerol (> 99.5%, Sigma-Aldrich, US), sucrose (> 99.5%, Pure Science), sodium hydroxide (> 97% ACS, BDH), Luria–Bertani (LB Broth, Fort Richard).

2.2 AuNP synthesis

Citrate-stabilised AuNPs were synthesised as previously published by Piella et al. [18]. All glassware was cleaned with aqua regia, rinsed with milli-Q water and dried in the oven. One hundred fifty millilitres sodium citrate solution (2.2 mM) with 0.1 mL of tannic acid (2.5 mM) and 1 mL of potassium carbonate (150 mM) were mixed and heated to 70 °C in a three-necked round bottom flask. Once the desired temperature was reached (70 °C), 1 mL of tetrachloroauric acid (25 mM) was injected, and a colour change was observed from clear to red–orange within 2 min. The reaction was allowed to proceed for another 5 min at 70 °C. The solution was cooled to room temperature, and the 5 nm AuNPs were isolated by centrifugation at 25,000*g* for 20 min.

2.3 Bacterial culture and OMV isolation

Pseudomonas aeruginosa PA01 (ATCC 15692) was obtained from Washington State University (Pullman, Washington, USA). Bacteria were cultured in standard Luria–Bertani (LB broth, 100 mL) at 37 °C for 18 h with aeration in large conical flasks. Overnight cultures were diluted 1:100 in fresh LB media and grown for 4 h to allow them to reach exponential phase prior to use. An overnight culture was diluted to an OD600 of 0.01 in LB and grown with aeration at 37 °C for 24 h. The media was collected and centrifuged twice at 10,000*g* for 30 min, followed by filtration through a 0.45 µm syringe filter (Millipore, Merck, US). The collected vesicles in media were then passed through a 0.22-µm filter, and OMVs were purified using two different methods. The first method was using a size exclusion column (qEV, Izon, New Zealand) after which they were concentrated and resuspended in Milli-Q water using the 30 kDa Amicon spin filters. The second OMV isolation method used ultracentrifugation for 1 h at 100,000 g to pellet the vesicles after which the pellet was resuspended in water. The resuspended OMVs were then ultracentrifuge again for 1 h at 100,000 g. The pellet was resuspended in Milli-Q water, and OMVs were cleaned and concentrated using 30 kDa Amicon spin filters. The OMVs isolation method used here follows the Minimal Information for Studies of Extracellular Vesicles (MISEV) guidelines [19].

2.4 Protein concentration of OMVs

Absorbance by proteins is primarily due to the aromatic rings of phenylalanine, tyrosine, and tryptophan residues that is why a UV absorbance at 280 nm can be used to determine protein concentrations. Nanodrop ND-1000 spectrophotometer was used to determine the concentration of proteins in the previously isolated OMVs using absorbance at 280 nm.

2.5 Transmission electron microscope

The size and shape of AuNPs were determined using TEM; 200 kV JEOL 2100F (JEOL, Tokyo, Japan). Five microlitres of as-purified AuNPs was pipetted onto the carbon-coated 300-mesh copper grids. Excess AuNP solution was removed after 30 min of adsorption, and the sample grid was allowed to dry for another 30 min.

OMV TEM samples were prepared by first plasma (oxygen) treating the carbon-coated copper TEM grids for 5 min, pipetting 5 µL of OMV solution onto the grid. After 5 min, the excess sample was removed, and 5 µL of 4% uranyl acetate was used to stain the sample for 6 min and subsequently washed three times with Milli-Q water. The morphology and size of OMVs were characterised, and all images were analysed using Gatan Microscopy Suite Software (GMS 3).

2.6 Dynamic light scattering

The hydrodynamic diameter and zeta potential of OMVs and AuNPs were determined using a Malvern Zetasizer ZS90 (Malvern Instruments, UK). A solution of AuNPs/electroporation buffer (1:1, *v*/*v*) was made, to obtain 200 µL samples for each electroporation voltage from 0.00, 0.40, 0.47, 0.80, 1.20 and 1.5 kV. The samples were then centrifuged, filtered and resuspended in 900 µL of milli-Q water. A similar process was followed for the OMVs samples, but with an OMV solution/electroporation buffer ratio of 1:3, *v*/*v*.

2.7 UV/vis spectroscopy

The absorbance of OMVs and AuNPs samples was measured using a Varian Cary50 Bio UV–Vis Spectrophotometer. Measurements were obtained using a two-sided glass cuvette. Solutions of AuNPs/electroporation buffer (1:1, *v*/*v*) were made to obtain 200 µL samples for each electroporation voltage (0.00, 0.40, 0.47, 0.80, 1.20 and 1.5 kV). Samples were centrifuged, filtered and resuspended in 700 µL of milli-Q water.

2.8 Electroporation of OMVs

Electroporation of OMVs was done using a Bio-Rad micropulser electroporator. The electroporation buffer was prepared by mixing 10% glycerol with 500 mM sucrose after which the pH was adjusted to 7.0 using few drops of sodium hydroxide solution. Electroporation voltage and concentration conditions were optimised by first electroporating OMVs alone by adding 50 µL of OMVs with 100 µL milli-Q water and 50 µL of electroporation buffer to obtain a total volume of 200 µL. For samples with the AuNPs, 50 µL of OMVs was added to a solution of 100 µL of AuNP and 50 µL of electroporation buffer to obtain a total volume of 200 µL. Each sample was electroporated at different voltages (0.00, 0.40, 0.47, 0.80, 1.20 and 1.5 kV). The samples were then centrifuged, filtered and concentrated. An optimal voltage of 0.47 kV and 1 pulse was selected as this showed minimal damage. Figure 1 shows schematically the steps followed to load the AuNPs into the OMVs, from a bacterial culture to a loaded OMV.

3 Results and discussion

Pseudomonas aeruginosa (POA1) were cultured to the exponential phase as it is the most uniform phase in terms of chemical and physical properties and allows sufficient OMV Production. It is important to note that previous studies determined that OMVs derived from bacteria at the exponential phase result in a lower quantity of OMVs but are considered the best in terms of stability [20]. The exponential phase represents a steady state where most of the cell properties are constant [21]. OMVs during this phase contain lower concentrations of some substances such as metals than in the stationary phase [22].

Once the media is collected, excess cells and cell debris were removed using centrifugation. This was done immediately after culture to ensure there was no contamination that can occur upon cell death. The supernatant was then passed through filters to remove larger micro-vesicles. OMVs were purified using ultracentrifugation and size exclusion chromatography, which are commonly used to purify of extracellular vesicles. Subsequent characterisation of OMVs was done using TEM (Fig. 2) and cryo-SEM (Fig. 3) showing spherical particles of sizes ranging from 30 to 200 nm. TEM and cryo-SEM images also demonstrated fully intact vesicles with no evidence of holes or damage on the surface due to the electroporation. Here we compared the common isolation methods: (1) ultracentrifugation and (2) size exclusion chromatography, and both methods showed a similar sized OMVs but differed in protein content. The OMVs isolated by ultracentrifugation contained higher concentrations of proteins ranging from 0.27 to 0.80 mg/mL, compared to 0.08–0.21 mg/mL for OMVs isolated by size exclusion chromatography. The TEM images also show higher-purity OMVs from the size

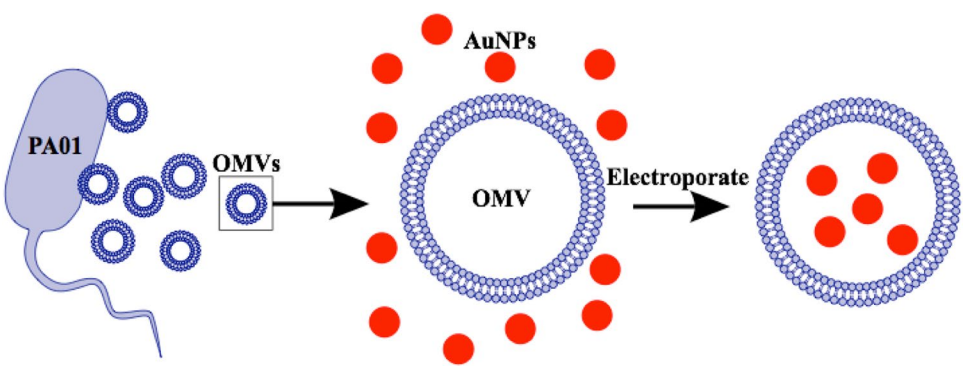

Fig. 1 Schematic representation of the electroporation of OMVs to load AuNPs. PA01 (*Pseudomonas aeruginosa*), OMV (outer membrane vesicle), AuNPs (gold nanoparticles)

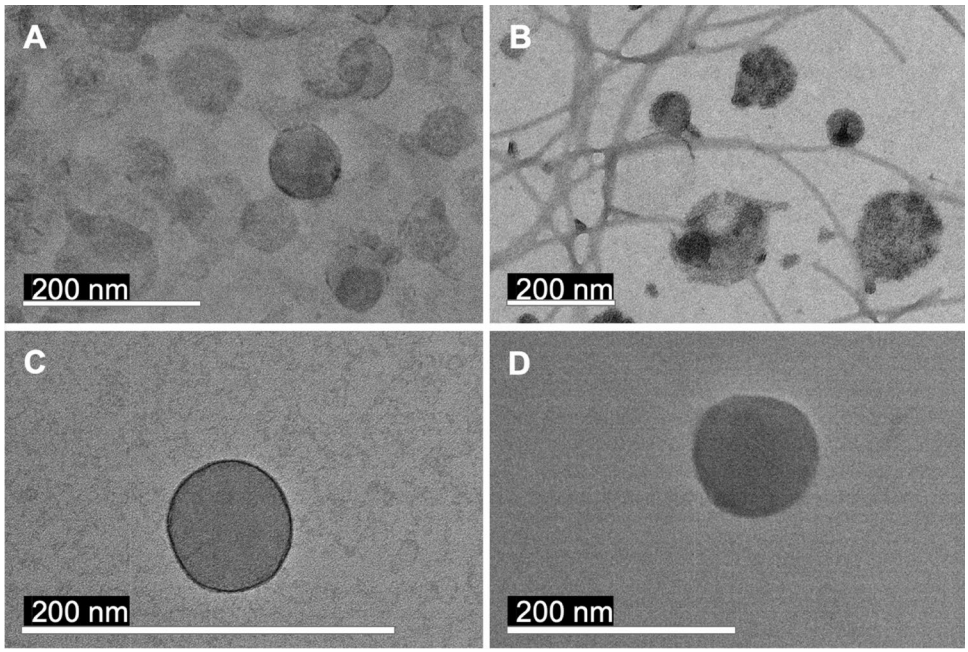

Fig. 2 TEM images of PA01 derived OMVs using ultra-centrifugation (**a**, **b**) and size exclusion chromatography (**c**, **d**)

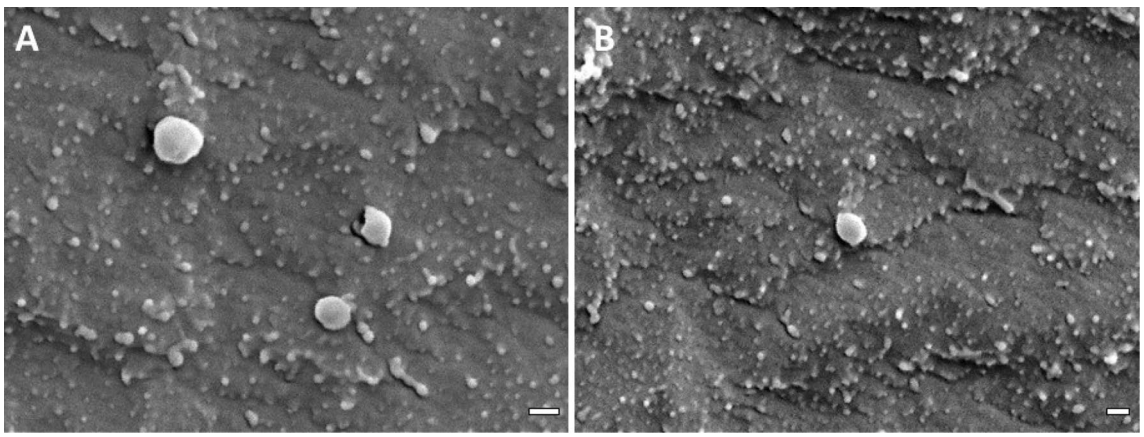

Fig. 3 Cryo-SEM images of PA01 derived OMVs. Scale bar represents 100 nm

exclusion chromatography with no impurities or any cell debris. It is agreed that ultracentrifugation doesn't eliminate cell impurities such as pili and flagella, and it is usually combined with a density gradient as a purification step for the OMVs. With that said, size exclusion chromatography produce more dilute samples [23]. Therefore, an extra step was added to concentrate the samples using molecular weight cut-off centrifugal filters.

Ultra-small AuNPs (< 10 nm) were synthesised using a previously reported method by Piella et al. [18]. The synthesis produced citrate-stabilised nanoparticles smaller than 10 nm in size. AuNPs were characterised using TEM (Fig. 4a) where the average size was measured at ~ 7 nm (Fig. 4b) and the distance between the lattice fringes was 0.233 nm (Fig. 4 inset; Au 111), which corresponds to previous reports that use this synthesis [24]. The size of the AuNP was important for the subsequent step of electroporation where only particles of < 10 nm can enter the OMVs. A previous study revealed that the pores formed in the plasma membrane generated during electroporation were only 1–10 nm [25]. The pore radius depends on the voltage, the number of pulses, pulse duration, the size of the OMVs and the cuvette size. It is possible to create large pores by controlling these parameters, but larger pores can lead to irreversible vesicle rupture.

AuNPs have been shown to be an affective nanomaterial for biomedical applications, including drug delivery [26]. The surface of AuNPs can be easily functionalised to incorporate a diverse array of molecules, such as doxorubicin or paclitaxel for cancer treatments [27, 28]. However,

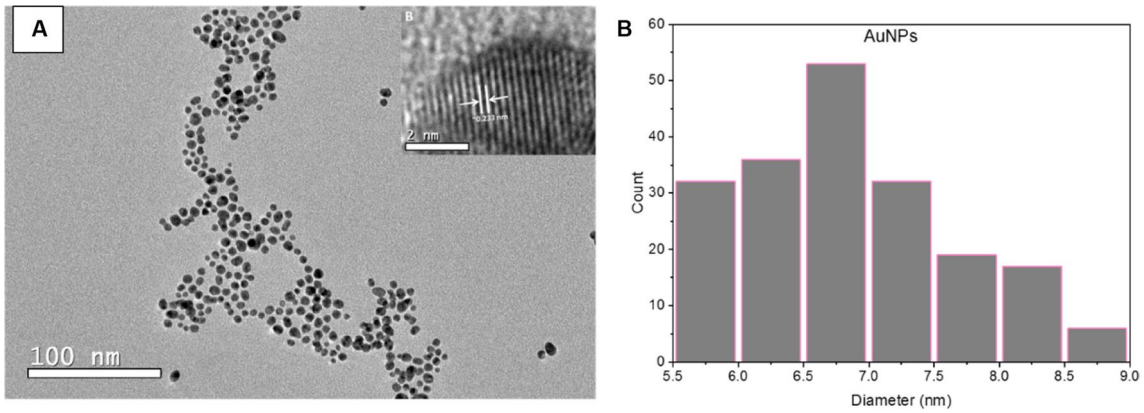

Fig. 4 TEM image (**a**) and size distribution (**b**) of spherical AuNPs and HR images showing the distance between two lattice fringes (~0.233 nm: (Au 111))

Table 1 Hydrodynamic diameter and zeta potential of OMVs with various voltages (0–1.5 kV)

Voltage (kV)	Electric field (V/m)	Zeta (− mV)	DLS (nm)
0.00	0.00	21.1 ± 3.5	192.0 ± 39.6
0.40	4.0×10^5	22.0 ± 2.4	206.4 ± 50.1
0.47	4.7×10^5	21.2 ± 2.1	146.0 ± 42.0
0.80	8×10^5	21.1 ± 2.2	202.4 ± 44.3
1.20	1.2×10^6	19.8 ± 1.4	203.6 ± 41.2
1.50	1.5×10^6	20.5 ± 3.5	193.8 ± 60.6

these ligand exchange procedures can cause changes in the size of nanoparticles which will influence their loading efficiency into OMVs. Also influences on toxicity must be carefully studied. Although it was reported that AuNPs are inherently non-toxic, some toxicity may be specific to certain ligands such as cationic ligands [29].

Electroporation of OMVs was optimised by varying the electric field by maintaining a constant cuvette width and varying the voltage. As expected, increasing the voltage resulted in OMV damage, which was shown by the decrease in absorption (Figure S1A) at 280 nm (representative of protein). There was also an increase in standard deviation of the hydrodynamic size of the OMVs from 192.0 ± 39.6 nm (0 kV) to 193.8 ± 60.6 nm (1.5 kV) (Table 1). This indicates that the OMVs stability was disrupted at 1.5 kV, disturbing the bilayer membrane. An optimum voltage was established (0.47 kV) to maintain OMV and AuNP integrity and was subsequently used for the electroporation of AuNPs into the purified OMVs. The stability of the AuNP was verified by monitoring the absorption peak for AuNP at 520 nm. This remained unchanged before and after electroporation (Figure S2B), meaning that no AuNP agglomeration occurred. Once the AuNPs and OMVs were mixed and electroporated, the excess AuNPs were removed using molecular weight cut-off centrifugal filters.

Zeta potential and hydrodynamic size of OMVs mixed with AuNPs (not electroporated) and OMVs with AuNPs electroporated and washed were measured. As shown in Table 2, there was no significant change in surface charge between the OMVs (− 21.2 mV) and the OMVs loaded with AuNP (− 20.4 mV). This suggested that the properties of the OMVs were well preserved after electroporation, therefore preserving their ability to properly stimulate an immune response and to target specific cells and tissues. Similar results also were observed for the OMVs mixed with AuNP without any electroporation, which showed zeta values of − 20.1 mV. This is consistent with the work of Zhao et al. [16] where exosomes were electroporated and the zeta potential showed similar results for before and after electroporation.

Table 2 Hydrodynamic diameter and zeta potential of (i) OMVs and AuNPs without electroporation, (ii) electroporated OMVs and (iii) OMVs and AuNPs electroporated

	Voltage (kV)	Electric field (V/m)	Zeta (− mV)	DLS (nm)
(i) OMVs/AuNPs without electroporation	0.00	0.00	20.1 ± 1.2	163.5 ± 33.2
(ii) OMVs	0.47	4.7×10^5	21.2 ± 2.1	146.0 ± 42.0
(iii) OMVs/AuNPs with electroporation	0.47	4.7×10^5	20.4 ± 1.5	140.2 ± 55.3

TEM images were collected of OMVs loaded with AuNPs that were negatively stained with uranyl acetate (Fig. 5a, b). Fringes were observed for uranyl acetate (> 0.33 nm) and for the AuNPs loaded inside (0.233 nm (Au 111); Fig. 5b inset). Cryo-SEM was used to compare isolated OMVs with no AuNPs (Fig. 5c, d). There were no noticeable differences observed on the surface of the OMVs, as shown below, which was a further indication of a successful loading of the nanoparticles into the vesicles (Fig. 5c, d).

Scanning transmission electron microscopy (STEM) and energy-dispersive X-ray spectroscopy (EDS) mapping was performed on OMVs loaded with AuNPs. An elemental map of the elements of interest was done as shown in Fig. 6, Au (green), O (red) and U (pink) confirming the presence of gold in the same area as the OMV. Other elemental maps were done and included in Figure S2, showing an AuNP of about 3 nm in size to be trapped inside an OMV. With a combination of DLS and TEM results, we confirm that the AuNPs are encapsulated inside the OMVs and that the electroporation is an efficient method for loading nanoparticles into vesicles. In Figure S4, the absorbance spectra of OMVs and AuNPs before and after electroporation using the same concentrations show a significant decrease in the AuNPs absorbance peak at around 520 nm from 0.11 to 0.09 suggesting around 20% of AuNPs were destroyed from electroporation. These results were compared with the supernatant discarded during the washing step suggesting that 45% of the AuNPs were in excess and therefore lost in the washing. The remaining 35% of the initial amount of AuNPs is assumed to be encapsulated into OMVs.

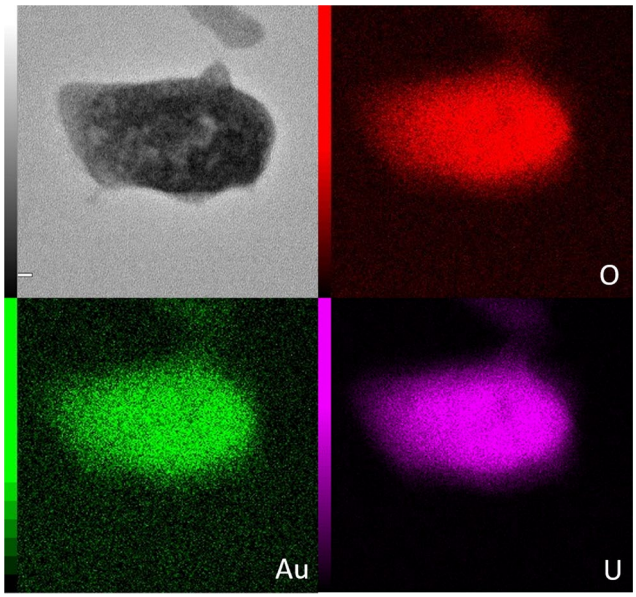

Fig. 6 STEM–EDS images of an OMV filled with AuNPs and stained with uranyl acetate with an elemental map for Au (green), O (red) and U (pink)

In their native form, OMVs contain high amounts of lipopolysaccharides (LPS) that can elicit immune responses; thus, several studies have been done to modify bacterial strains into detoxified LPS to reduce the

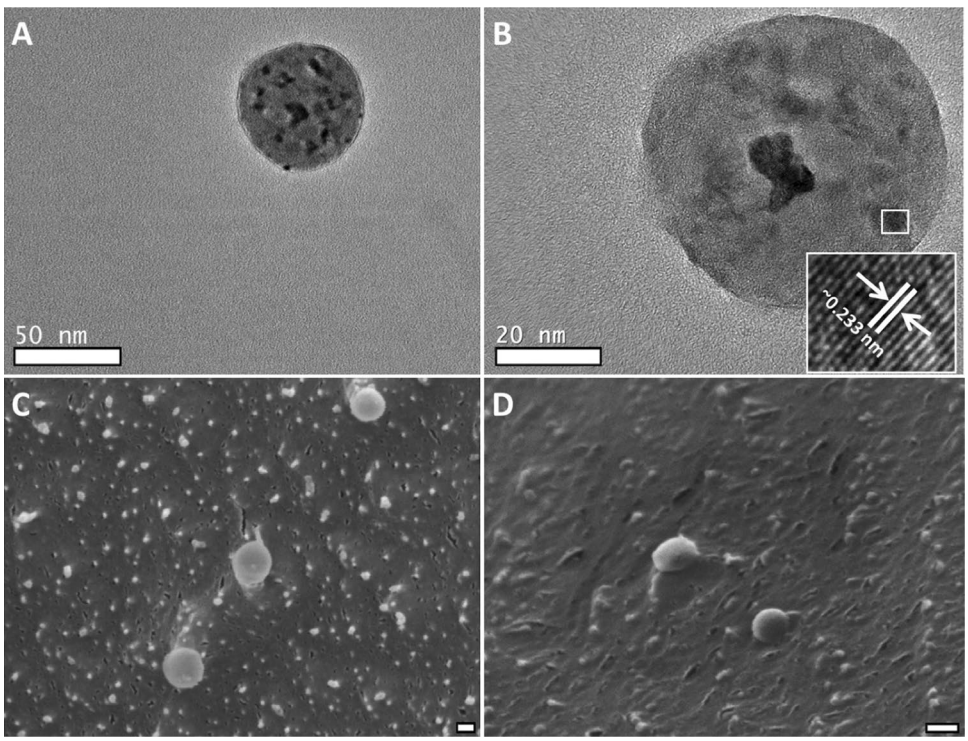

Fig. 5 TEM images (**a**, **b**) and cryo-SEM images (**c**, **d**) of PA01 derived OMVs loaded with AuNPs. Inset shown in **b** shows lattice fringe distances of 0.233 nm (Au 111). Scale bar (**c**, **d**) represents 100 nm

endotoxicity of OMVs [30]. In addition, the findings of Dauros Singorenko et al. [31] have shown that samples purified using size exclusion chromatography contained lower amounts of LPS when compared to the crude sample. For further verification, cytotoxicity studies of the system developed here are planned for future work. Advance studies might include the delivery of OMVs to bacterial cells to observe the delivery point of the AuNPs.

4 Conclusion

In conclusion, AuNPs were successfully synthesised and electroporated inside OMVs which was verified using DLS, TEM and Cryo-SEM. The stability of the OMVs after electroporation was monitored using DLS and electron microscopy to ensure that the OMV integrity was maintained. Minimal change in the hydrodynamic diameter of the OMVs, as well as the localisation of the nanoparticles inside the vesicles, was observed, which confirmed the incorporation of AuNPs into the OMVs. This approach could be adapted to include a suite of other functional nanomaterials, further opening up promising avenues for drug delivery in vivo. Although small nucleic acid such as siRNAs have been successfully loaded into OMVs, so far none of the studies have reported using electroporation to load nanoparticles. Our study remains the first to successfully encapsulate nanoparticles inside an OMV.

Acknowledgements The authors would like to acknowledge David Flynn for his expertise on the use of the TEM. Thanks are due to Claudia Brosnahan-Couturier (Bordeaux INP Enseirb Matmeca) who organised Luana Cuvillier's internship.

Author's contribution RG and ZA helped in conceptualisation; RG and ZA contributed to methodology; LC, ZA, GD and RVG helped in validation; ZA, GD and RG were involved in formal analysis; LC and ZA helped in investigation; RG contributed to resources; LC, ZA and RG were involved in data curation; RG, ZA and GD contributed to writing—original draft preparation; RG, GD and ZA were involved in writing—review and editing; RG and ZA helped in visualisation; RG contributed to supervision; RG helped in project administration; RG helped in funding acquisition.

Compliance with ethical standards

Conflict of interest The authors declare no conflict of interest.

References

1. Kakkar A, Traverso G, Farokhzad OC et al (2017) Evolution of macromolecular complexity in drug delivery systems. Nat Rev Chem 1:0063. https://doi.org/10.1038/s41570-017-0063
2. Derfus AM, Chen AA, Min D-H et al (2007) Targeted quantum dot conjugates for siRNA delivery. Bioconjug Chem 18:1391–1396. https://doi.org/10.1021/BC060367E
3. Wang F, Wang Y-C, Dou S et al (2011) Doxorubicin-tethered responsive gold nanoparticles facilitate intracellular drug delivery for overcoming multidrug resistance in cancer cells. ACS Nano 5:3679–3692. https://doi.org/10.1021/nn200007z
4. Ménard-Moyon C, Venturelli E, Fabbro C et al (2010) The alluring potential of functionalized carbon nanotubes in drug discovery. Expert Opin Drug Discov 5:691–707. https://doi.org/10.1517/17460441.2010.490552
5. Wang Q, Zhuang X, Mu J et al (2013) Delivery of therapeutic agents by nanoparticles made of grapefruit-derived lipids. Nat Commun 4:1867. https://doi.org/10.1038/ncomms2886
6. de la Torre Gomez C, Goreham RV, Bech Serra JJ et al (2018) "Exosomics"—a review of biophysics, biology and biochemistry of exosomes with a focus on human breast milk. Front Genet 9:92. https://doi.org/10.3389/fgene.2018.00092
7. Dobhal G, Ayupova D, Laufersky G et al (2018) Cadmium-free quantum dots as fluorescent labels for exosomes. Sensors 18:3308. https://doi.org/10.3390/s18103308
8. Tian T, Zhang H-X, He C-P et al (2018) Surface functionalized exosomes as targeted drug delivery vehicles for cerebral ischemia therapy. Biomaterials 150:137–149. https://doi.org/10.1016/j.biomaterials.2017.10.012
9. Gorringe A, Halliwell D, Matheson M et al (2005) The development of a meningococcal disease vaccine based on *Neisseria lactamica* outer membrane vesicles. Vaccine 23:2210–2213. https://doi.org/10.1016/j.vaccine.2005.01.055
10. Sun D, Zhuang X, Xiang X et al (2010) A novel nanoparticle drug delivery system: the anti-inflammatory activity of curcumin is enhanced when encapsulated in exosomes. Mol Ther 18:1606–1614. https://doi.org/10.1038/mt.2010.105
11. Zhuang X, Xiang X, Grizzle W et al (2011) Treatment of brain inflammatory diseases by delivering exosome encapsulated anti-inflammatory drugs from the nasal region to the brain. Mol Ther 19:1769–1779. https://doi.org/10.1038/mt.2011.164
12. Alvarez-Erviti L, Seow Y, Yin H et al (2011) Delivery of siRNA to the mouse brain by systemic injection of targeted exosomes. Nat Biotechnol 29:341–345. https://doi.org/10.1038/nbt.1807
13. Shtam TA, Kovalev RA, Varfolomeeva E et al (2013) Exosomes are natural carriers of exogenous siRNA to human cells in vitro. Cell Commun Signal 11:88. https://doi.org/10.1186/1478-811X-11-88
14. Wahlgren J, Karlson TDL, Brisslert M et al (2012) Plasma exosomes can deliver exogenous short interfering RNA to monocytes and lymphocytes. Nucleic Acids Res 40:e130–e130. https://doi.org/10.1093/nar/gks463
15. Tian Y, Li S, Song J et al (2014) A doxorubicin delivery platform using engineered natural membrane vesicle exosomes for targeted tumor therapy. Biomaterials 35:2383–2390. https://doi.org/10.1016/j.biomaterials.2013.11.083
16. Zhao J-Y, Chen G, Gu Y-P et al (2016) Ultrasmall magnetically engineered Ag_2 Se quantum dots for instant efficient labeling and whole-body high-resolution multimodal real-time tracking of cell-derived microvesicles. J Am Chem Soc 138:1893–1903. https://doi.org/10.1021/jacs.5b10340
17. Hood JL, Scott MJ, Wickline SA (2014) Maximizing exosome colloidal stability following electroporation. Anal Biochem 448:41–49. https://doi.org/10.1016/j.ab.2013.12.001

18. Piella J, Bastús NG, Puntes V (2016) Size-controlled synthesis of Sub-10-nanometer citrate-stabilized gold nanoparticles and related optical properties. Chem Mater 28:1066–1075. https://doi.org/10.1021/acs.chemmater.5b04406
19. Théry C, Witwer KW, Aikawa E et al (2018) Minimal information for studies of extracellular vesicles 2018 (MISEV2018): a position statement of the International Society for Extracellular Vesicles and update of the MISEV2014 guidelines. J Extracell Vesicles 7:1535750. https://doi.org/10.1080/20013078.2018.1535750
20. Henry T, Pommier S, Journet L et al (2004) Improved methods for producing outer membrane vesicles in gram-negative bacteria. Res Microbiol 155:437–446. https://doi.org/10.1016/j.resmic.2004.04.007
21. Monod J (1949) The growth of bacterial cultures. Annu Rev Microbiol 3:371–394
22. Tashiro Y, Ichikawa S, Shimizu M et al (2010) Variation of physiochemical properties and cell association activity of membrane vesicles with growth phase in *Pseudomonas aeruginosa*. Appl Environ Microbiol 76:3732–3739. https://doi.org/10.1128/AEM.02794-09
23. Welton JL, Webber JP, Botos LA et al (2015) Ready-made chromatography columns for extracellular vesicle isolation from plasma. J Extracell Vesicles 4:1–9. https://doi.org/10.3402/jev.v4.27269
24. Karuppasamy L, Chen CY, Anandan S, Wu JJ (2017) High index surfaces of Au-nanocrystals supported on one-dimensional MoO_3-nanorod as a bi-functional electrocatalyst for ethanol oxidation and oxygen reduction. Electrochim Acta 246:75–88. https://doi.org/10.1016/j.electacta.2017.06.040
25. Krassowska W, Filev PD (2007) Modeling electroporation in a single cell. Biophys J 92:404–417. https://doi.org/10.1529/biophysj.106.094235
26. Cai W, Gao T, Hong H, Sun J (2008) Applications of gold nanoparticles in cancer nanotechnology. Nanotechnol Sci Appl 1:17–32
27. Gibson JD, Khanal BP, Zubarev ER (2007) Paclitaxel-functionalized gold nanoparticles. J Am Chem Soc 129:11653–11661. https://doi.org/10.1021/ja075181k
28. Aryal S, Grailer JJ, Pilla S et al (2009) Doxorubicin conjugated gold nanoparticles as water-soluble and pH-responsive anticancer drug nanocarriers. J Mater Chem 19:7879–7884. https://doi.org/10.1039/b914071a
29. Goodman CM, McCusker CD, Yilmaz T, Rotello VM (2004) Toxicity of gold nanoparticles functionalized with cationic and anionic side chains. Bioconjug Chem 15:897–900. https://doi.org/10.1021/bc049951i
30. van der Ley P, van den Dobbelsteen G (2011) Next-generation outer membrane vesicle vaccines against *Neisseria meningitidis* based on nontoxic LPS mutants. Hum Vaccin 7:886–890. https://doi.org/10.4161/hv.7.8.16086
31. Dauros Singorenko P, Chang V, Whitcombe A et al (2017) Isolation of membrane vesicles from prokaryotes: a technical and biological comparison reveals heterogeneity. J Extracell Vesicles 6:1324731. https://doi.org/10.1080/20013078.2017.1324731